Fifth International Conference on Numerical Methods in Geomechanics / Nagoya / 1-5 April 1985

Numerical modelling of interfaces using conventional finite elements

D.V.GRIFFITHS
University of Manchester, UK

ABSTRACT: The ability of eight-noded quadrilateral elements to model interface phenomena is examined. The elements are tested for both adhesive and frictional sliding for various values of stiffness and aspect ratio. It was found that the elements often performed well, but for higher aspect ratios, a tighter convergence criterion was necessary.

1. INTRODUCTION

Interface behaviour is characterised by large relative movement occurring over a short distance once a threshold force or stress level is reached. The use of interface finite elements to model slippage of this kind is quite well established, and specialised elements have been developed (Goodman et al 1968) Applications have usually involved modelling soil/structure interface behaviour such as in jointed rock masses, footings, piles and buried steel culverts (Desai and Holloway 1972, Chung and Lee 1972, Ghaboussi et al 1973, Desai 1974, Chow 1981, Katona 1983. Desai et al 1984). Other authors have proposed the use of conventional isoparametric finite elements to model interface behaviour (Zienkiewicz et al 1970, Pande and Sharma 1979, Chin 1979, de Borst and Vermeer 1982) which included recommendations that the interface stiffness be reduced relative to the surrounding medium to allow large relative movement.

If specialised elements are to be used to model slippage two questions may be asked before proceeding -

a)Is accurate modelling of slippage essential to the analysis?

b)Is the use of specialised elements to model interface behaviour justified on the grounds of accuracy, efficiency, convenience, etc.?

Point a) is not always easy to answer in advance. In such cases it may be necessary to include interfaces, even at the risk of them not having much influence on the main physical points under investigation.

Point b) aims to minimise the complexity of a particular finite element analysis. Although changing element type within a mesh of elements is quite easily done in experienced hands, it is clearly preferable to use the same type of element throughout if possible.

The 6-noded interface element, for example, has been shown to be effective in modelling slippage in conjunction with 8-noded elements (Willson 1984) but the 8-noded element itself has by no means been ruled out. Pande and Sharma (1979) proposed the use of thin 8-noded quadratic elements enabling a linear variation of strain across the joint. These authors also compared the ability of this element using both absolute and relative displacement functions (Wilson 1977). It was found that the conventional approach gave satisfactory results up to very high aspect ratios provided the computer had sufficient word length (36 bit word).

The aim of this paper is to look further into the use of the 8-noded quadratic element when used to model slippage. The content is more 'experimental' than 'theoretical', and conclusions are drawn from observed behaviour in several numerical experiments.

Initially, simple problems are

considered for calibration purposes using both frictional and adhesive models. Parametric studies of aspect ratio, relative stiffness and plasticity convergence criterion are performed. Subsequently the elements are tested in actual boundary-value problems of laterally loaded foundations and earth pressure.

The performance of the interface elements is generally considered from the viewpoint of their load-displacement behaviour. In all cases, the elements are assumed to be elastic/perfectly plastic, and conventional iterative methods (Zienkiewicz 1977, Smith 1982) have been used to model the non-linearity.

2. CASE 1 - PLANE STRAIN ANALYSIS OF INCLINED INTERFACES

The problem to be analysed is shown in figure 1.

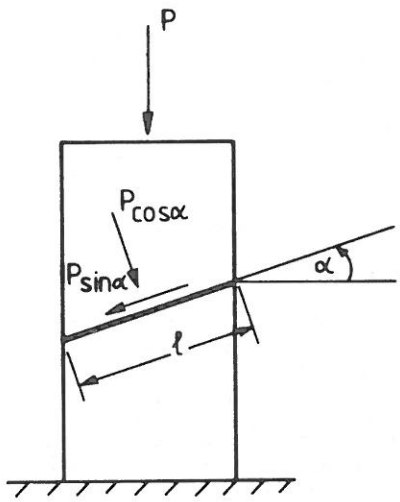

Figure 1 Axially loaded column

The column contains an inclined interface of weak material, and the axial force is to be increased until irreversible slippage occurs. From simple statics, the value of P at failure is given as follows:-

2.1 Friction

If the interface obeys a simple frictional law with a limiting friction angle given by ϕ, then slippage occurs when the inclination of the interface is given by -

$$\alpha = \phi \qquad (1)$$

Note that failure in this case does not depend on the magnitude of P.

2.2 Adhesion

If the interface is adhesive with a shear strength of C_w, then slippage occurs when

$$P\sin\alpha = \ell C_w \qquad (2)$$

Assuming the column (figure 1) is of unit width gives

$$\ell = \frac{1}{\cos\alpha}$$

hence $$P_{ult} = \frac{C_w}{\sin\alpha\cos\alpha} \qquad (3)$$

Table 1 shows the value of the ratio P_{ult}/C_w for a range of α-values.

Table 1. Axial force to cause slip with an adhesive interface

α	P_{ult}/C_w
10 or 80	5.85
20 or 70	3.11
30 or 60	2.31
40 or 50	2.03
45	2.00

2.3 Finite element analysis

Finite element analysis of the problem was performed using the mesh of figure 2.

The program data was arranged so that the interface thickness, inclination and properties could be easily varied. Plastic yielding, if it was to occur, was concentrated on the inclined element by giving the elements above and below very high strengths. Although the mesh of figure 2 is similar to the one used by Pande and Sharma (1979), the present work allows unrestrained sliding along the interface and includes no line of symmetry.

Before considering elasto/plastic behaviour, the purely elastic response of the mesh to axial loading was observed to ensure that the displacement pattern was reasonably uniform in spite of the asymmetric mesh. Although a small degree of non-uniform deformatiom was computed along the top of the mesh, the effect was small enough to be of little consequence.

2.4 Results

For both the frictional and adhesive cases, parametric studies were

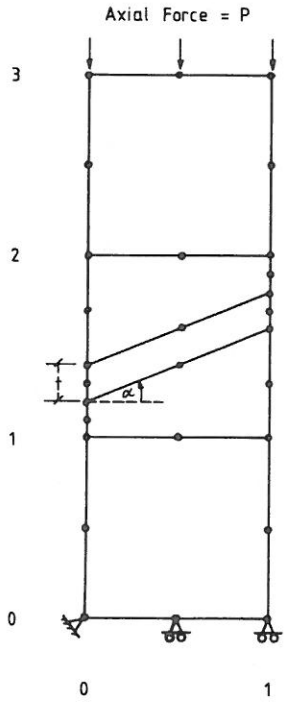

Figure 2 Mesh of 8-noded elements for study of inclined interfaces.

concentrated on a) The interface aspect ratio (defined 1/t) b) The ratio of Young's modulus in the interface E_i to that in the surrounding medium E and c) The convergence tolerance employed in the elasto/plastic iterative algorithm.

Figure 3 (i), (ii) and (iii) shows results for the adhesive case for three different interface inclinations. These results were all obtained using the same interface stiffness and convergence tolerance. In each case, the axial load was increased incrementally and the corresponding axial displacement computed. The analytical solutions from Table 1 are also shown for comparison. Two main factors emerge - firstly the interface with an aspect ratio of 10 reproduced sliding behaviour along an

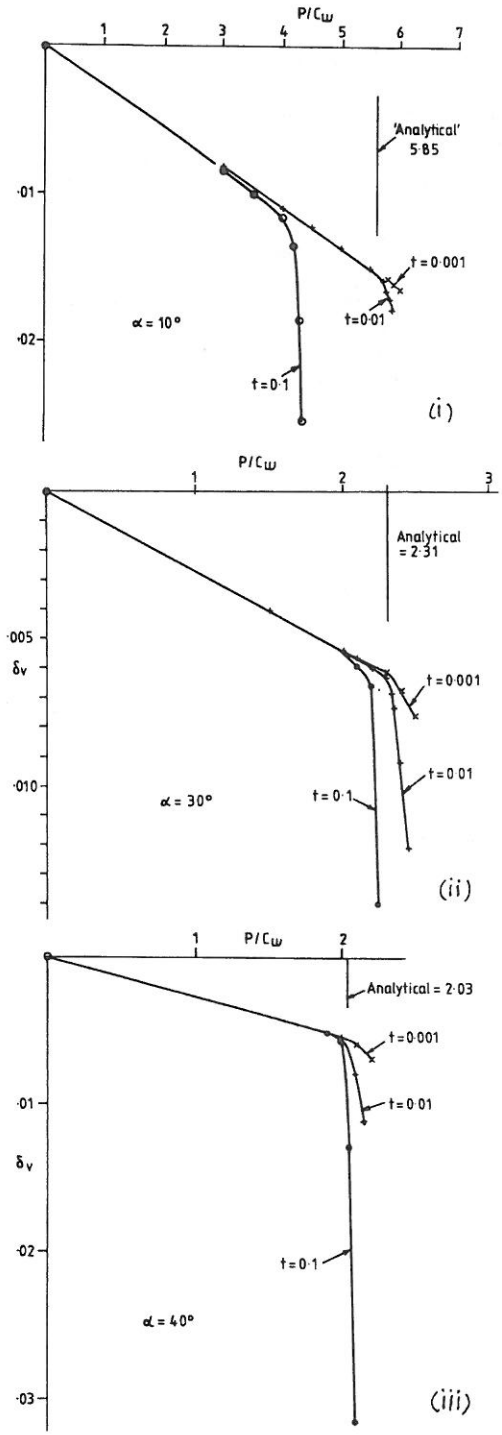

Figure 3 Computed load v displacement for different interface inclinations

inclined interface quite well although increasingly conservatively as the interface inclination was decreased. Secondly, for higher aspect ratios of 100 and especially 1000, over-stiff behaviour was obtained with less convincing modelling of sliding. In these cases, reducing Young's modulus in the interface seemed to make little difference.

The frictional case was possibly an even more severe test of interface response. In this case, the axial force was kept constant and the interface inclination, α , gradually increased until it approached the friction angle .

In general, similar behaviour to that occuring in the adhesive case was obtained. Yielding invariably commenced before α reached ϕ and the thicker the element the more conservative the slip behaviour predicted.

In the finite element program, 'constant stiffness' iterations were used to achieve a solution which did not violate the failure criterion. At each iteration, a set of self-equilibrating body-forces were generated. Convergence was satisfied if, at two consecutive iterations, none of the body-forces (non-dimensionalised by dividing by the one of largest magnitude) changed by more than the quantity "TOL".

For the thinner elements convergence became increasingly hard to achieve and there was a tendency for numerical 'drift' into illegal stress space. It is clear from figure 4 that for the frictional case with an aspect ratio of 100, a rather small tolerance was required to achieve a convincing sliding model. Furthermore, the higher the interface aspect ratio became, the tighter the tolerance had to be.

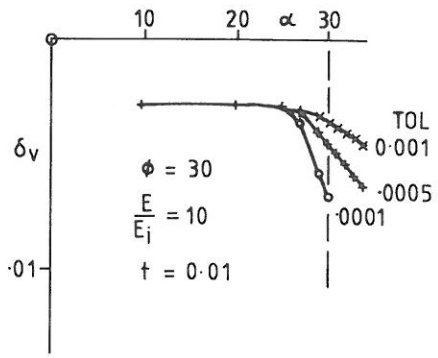

Figure 4. Effect of convergence tolerance on load v displacement.

Also for the frictional case, figure 5 shows the effect of reducing the interface stiffness relative to the surrounding medium. The load-deflection behaviour is seen to hardly change and the definition of failure not improved. The curve is merely shifted down by a constant amount due to the elastically softer interface element.

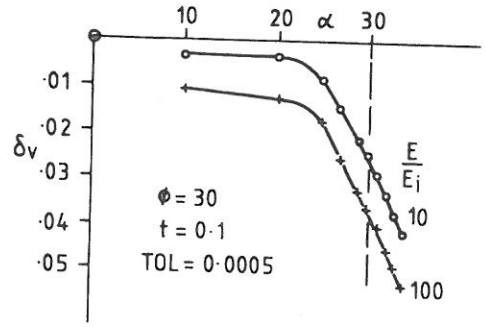

Figure 5 Influence of interface stiffness

3. CASE 2 LATERALLY LOADED FOOTING IN PLANE STRAIN

The mesh for this case is shown in Figure 6.

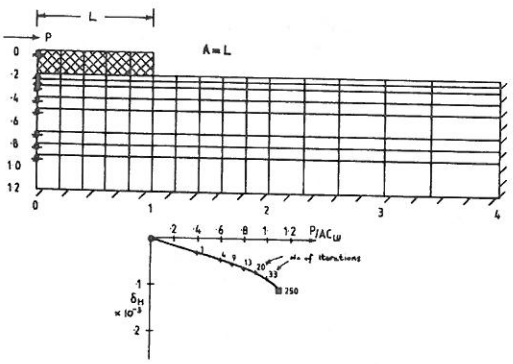

Figure 6 Mesh and load-deflection behaviour for laterally loaded footing in plane strain.

Eight-noded elements were used throughout and adhesive behaviour was assumed in the thin row of elements directly below the footing. In the case considered, the footing elements were

given high stiffness and strength, whereas the rest of the elements were given constant properties. Down the left side of the mesh vertical movement was prevented, implying an antisymmetric displacement field. Such a boundary condition is only possible with cylindrical failure criteria (von Mises, Tresca) which do not distinguish between compressive and tensile stress states.

A single horizontal force was applied to half the footing as shown and from inspection its ultimate value is given by

$$P_{ult} \not< LC_w \qquad (4)$$

where L is half the width of the footing and C_w the adhesion of the thin elements below. The inequality sign is necessary because the nearest point to the footing at which 'sliding' can be detected is at the first Gauss-point, which is a small but finite distance below. The eventual mechanism is thus of a 'tearing' rather than 'sliding' type and is bound to involve material beyond the edge of the footing.

Also shown in Figure 6 is the computed load displacement response. Failure was signalled by a dramatic increase in the number of iterations required by the algorithm for convergence. Indeed, in this case, convergence was not achieved within 250 iterations at a load which was around 10% higher than the pure sliding value. The displacement vectors of the mesh at failure are given in Figure 7, and this indicates the extent of the shallow tearing mechanism.

It may be pointed out, however, that in a continuum analysis such as this, it is impossible to model a truly localised failure mechanism (Griffiths 1982).

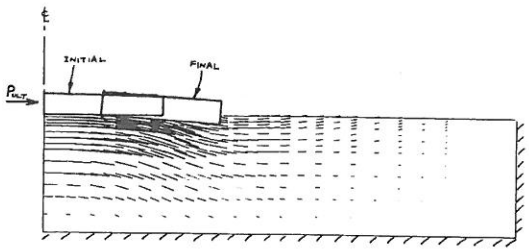

Figure 7 Displacement vectors at failure due to lateral loading

4. CASE 3 - LATERALLY LOADED CIRCULAR FOOTING

Although similar in character to the previous case this is a 3-dimensional problem, and as a consequence is considerably more complicated computationally. To avoid using a full 3-D finite element analysis the problem was solved as an axisymmetric body subjected to non-axisymmetric loads. An example of an elastic analysis of this type is given in Smith (1982) and present development by the author for elasto-plastic analyses is based on the method described by Winnicki and Zienkiewicz (1979). In brief, because of the axial symmetry of the problem, 2 - dimensional elements can be used in the radial planes, with variations in the circumferential direction dealt with using a Fourier series expansion.

A typical radial plane is given in Figure 8. The lateral loading, which itself takes the form of a 1st harmonic in a cosin series, is applied and the resulting load/deflection behaviour in the direction of loading is shown in Figure 9. A lower-bound on the computed lateral load at failure can be given as -

$$P_{ult} \not< \pi R^2 C_w \qquad (5)$$

where R is the radius of the footing and C_w the adhesion of the elements directly below.

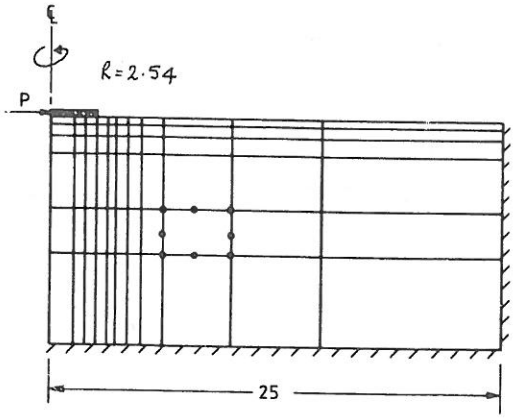

Figure 8 Mesh for laterally loaded circular footing

Many of the comments of the previous section are still valid. A tearing mode of failure is induced, but this time tearing can occur at all points around the

circumference of the footing. In the plane strain analysis, tearing could only occur directly in front and behind the footing. The results shown in Figure 9 were obtained using two (odd) harmonics only and stresses were monitored at circumferential positions corresponding to 0° (the direction of loading) 45°, 90°, 135° and 180°. A sudden failure was observed at a load which was approximately 20% higher than the pure sliding value.

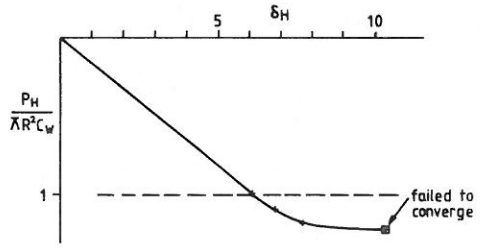

Figure 9 Load v displacement for laterally loaded circular footing.

Including more harmonics in the analysis would enable the spread of yield to be defined more accurately as it moves from the sides towards the front and back of the footing, but with correspondingly higher computer cost.

The so-called tearing mechanism is only obtained because the footing is resting, directly, on the soil surface. A better sliding result would be obtained if the interface only extended to the edge of the footing and not beyond (Figure 10).

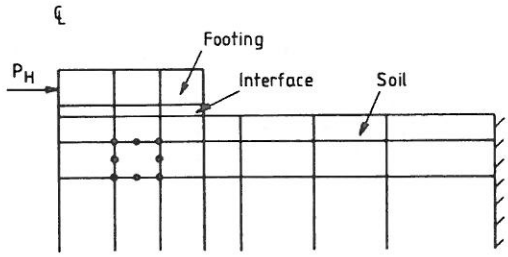

Figure 10 A better mesh for modelling pure sliding

5. CASE 4 EARTH PRESSURES - SMOOTH AND ROUGH WALLS

Earth pressure theory based on smooth walls is fairly straightforward and rigorous, bit if more realistic conditions of wall friction or adhesion are to be included only approximate solutions are available.

For example, in a cohesive soil with shear strength $\phi_u = 0$, C_u, the wall adhesion may vary in the range.

$$0 \leq C_w \leq C_u \qquad (6)$$

where $C_w = 0$ corresponds to smooth conditions. In the British Code of Practice on Earth Pressures (CP2), the maximum passive resistance of the soil to lateral wall movement is given by :-

$$P_p = \tfrac{1}{2} K_p \gamma H^2 + K_{pc} c H \qquad (7)$$

where γ, c and H are the soil's unit weight, cohesion and wall height respectively.

The recommended values of the coefficient K_{pc} are given in Table 2 :

Table 2 Factors for wall/soil adhesion

C_w/C_u	K_{pc}
0	2.0
0.5	2.4
1.0	2.6

A brief study of this problem was attempted using the mesh of figure 11 with a thin column of elements adjacent to the wall.

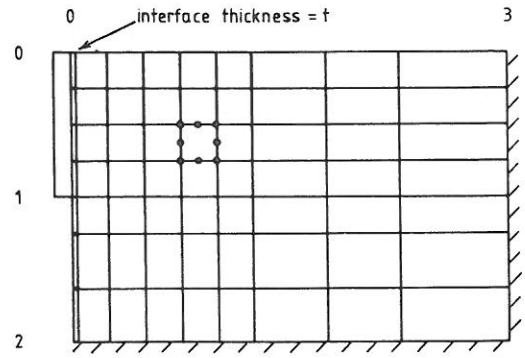

Figure 11 Mesh used for earth pressure analysis

No actual wall was included in the analysis, as loads were applied to the soil in the form of prescribed displacements. Wall 'roughness' was controlled by varying the adhesion of the

interface behind the wall while vertically restraining the displaced nodes. Smooth wall conditions (C_w = 0) were obtained by removing the interface and allowing unrestrained movement of the displaced nodes. The load corresponding to a given displacement of the wall was obtained by averaging the horizontal stresses in the interface and multiplying by the wall height (H=1).

Eliminating the first term of equation 7 by assuming the soil to be weightless, the results of figure 12 were obtained for three values of wall adhesion. The computed passive resistance ranged from the Rankine (smooth) value to the "rough" value (C_w = C_u) around 30% higher. The interfaces used to obtain these results had an aspect ratio of 10 and can be expected to be somewhat conservative. Further parametric studies on this problem are presently underway.

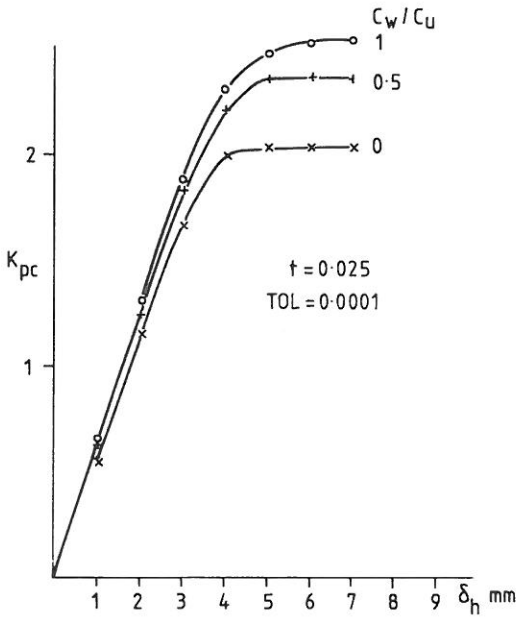

Figure 12. Build up of passive resistance for different values of wall adhesion

6. CONCLUSIONS

Thin eight-noded quadratic elements have been tested for their ability to model adhesive and frictional slippage. In the test-problem, it was found that an important parameter was the convergence tolerance used in the plasticity algorithm. As the element aspect ratio increased up to 1000, a much tighter tolerance was required than would be needed in normal usage of the elements. For smaller aspect ratios (up to 100), slippage was modelling quite accurately and increasingly conservatively.

The onset of slippage in the elements was apparent, not only from the increased shear displacements, but also from the sudden increase in iterations necessary for numerical convergence.

The boundary value problems performed well with failure occurring due to a shallow tearing mechanism rather than sliding. This resulted in failure loads that were 10-20% above the pure sliding value.

It is suggested that eight-noded elements could make satisfactory interfaces as a 'first approximation' or starting point for an analysis. If it is felt, however, that slippage is of prime concern in a given problem, then recourse to specialised elements may still prove necessary.

7. REFERENCES

de Borst, R. and Vermeer, P.A.1982. Finite element analysis of static penetration tests. Proc. 2nd European Symp. on Penetration testing, Amsterdam pp.457-462.

Chin, Y.K. 1979. Elasto-plastic finite element analysis in foundation engineering M.Sc. Thesis, Simon Engineering Labs., University of Manchester.

Chow, Y.K. 1981. Dynamic behaviour of piles. Ph. D. Thesis, Simon Engineering Labs., University of Manchester.

Chung, T.J. and Lee, J.K. 1972. Incremental plasticity theory applied to boundary value problems in soil. Proceedings, Symp. on Appl. of Finite Element meths in geotechnical engineering, Vicksburg, Mississippi.

Desai, C.S. 1974. Numerical design analysis for piles in sand. J. Geotech. Eng. Div., ASCE, v.100, No. GT6 pp 613-635.

Desai, C.S. and Holloway, D.M. 1972. Load deformation analysis of deep pile foundations. Proceedings, Symp. on Appl. of Finite Element meths. in geotechnical engineering. Vicksburg, Mississippi.

Desai, C.S., Zaman, M.M., Lightner, J.G. and Siriwardane, H.J. 1984. Thin layer element for interfaces and joints. Int. J. Num. Anal. Meths Geomech., v.8; pp. 19-43.

Ghaboussi, J., Wilson, E.L. and Isenberg J. 1973. Finite elements for rock and joint interfaces, J. Soil Mech. Found. Eng. Div., ASCE, v.99, No. SM10.

Goodman, R.E., Taylor, R.L. and Brekke T.L. 1968. A model for the mechanics of jointed rock. J. Soil Mech. Found Eng. Div., ASCE, v.94, No. SM3.

Griffiths, D.V. 1982. Computation of bearing capacity on layered soils. Proc. 4th Int. Conf. on Num. Meths. in Geomech. Edmonton, pp.163-170.

Katona, M.G. 1983. A simple contact friction interface element with applications to buried culverts. Int. J. for Num. Anal. Meths. Geomech., v.7; pp 371-384.

Pande, G.N. and Sharma, K.G. 1979. On joint/interface elements and associated problems of numerical ill - conditioning. Int. J. Num. Anal. Meths. Geomech., v.3; pp. 293-300.

Smith, I.M. 1982. Programming the finite element method, Chichester, U.K. John Wiley and Sons.

Willson, S.M. 1984. Finite element analysis of cone penetration. Ph. D. Thesis. Simon Engineering Labs., University of Manchester.

Wilson, E.L. 1977. Finite elements for foundations, joints and fluids, in Finite Elements in Geomechanics. ed. G. Gudehus, Ch.10. Chichester, John Wiley and Sons.

Winnicki, L.A. and Zienkiewicz, O.C. 1979. Plastic behaviour of axisymmetric bodies subjected to non-symmetric loading. Int. J. Num. Meths. Eng. v.14, pp.1399-1412.

Zienkiewicz, O.C. 1977. The finite element method 3rd ed., McCraw-Hill, Maidenhead.

Zienkiewicz, O.C., Best, B., Dullage, C. and Stagg, K.C. 1970. Analysis of non-linear problems in rock mechanics with particular reference to jointed rock systems. Proc. 2nd Cog. Intl. Soc. Rock Mech., Belgrade, pp. 8-14.